Comparison of ^{68}Ga-DOTANOC and ^{68}Ga-DOTATATE PET/CT Within Patients with Gastroenteropancreatic Neuroendocrine Tumors

Damian Wild[1,2], Jamshed B. Bomanji[1], Pascal Benkert[3], Helmut Maecke[2], Peter J. Ell[1], Jean Claude Reubi[4], and Martyn E. Caplin[5]

[1]Institute of Nuclear Medicine, University College Hospital, London, United Kingdom; [2]Division of Nuclear Medicine, Department of Radiology, University of Basel Hospital, Basel, Switzerland; [3]Clinical Trial Unit, University Basel Hospital, Basel, Switzerland; [4]Institute of Pathology, University of Berne, Berne, Switzerland; and [5]Neuroendocrine Tumour Unit, Royal Free Hospital, London, United Kingdom

Somatostatin receptor PET tracers such as [^{68}Ga-DOTA, 1-Nal^3]-octreotide (^{68}Ga-DOTANOC) and [^{68}Ga-DOTA,Tyr^3]-octreotate (^{68}Ga-DOTATATE) have shown promising results in patients with neuroendocrine tumors, with a higher lesion detection rate than is achieved with ^{18}F-fluorodihydroxyphenyl-L-alanine PET, somatostatin receptor SPECT, CT, or MR imaging. ^{68}Ga-DOTANOC has high affinity for somatostatin receptor subtypes 2, 3, and 5 ($sst_{2,3,5}$). It has a wider receptor binding profile than ^{68}Ga-DOTATATE, which is sst_2-selective. The wider receptor binding profile might be advantageous for imaging because neuroendocrine tumors express different subtypes of somatostatin receptors. The goal of this study was to prospectively compare ^{68}Ga-DOTANOC and ^{68}Ga-DOTATATE PET/CT in the same patients with gastroenteropancreatic neuroendocrine tumors (GEP-NETs) and to evaluate the clinical impact of ^{68}Ga-DOTANOC PET/CT. **Methods:** Eighteen patients with biopsy-proven GEP-NETs were evaluated with ^{68}Ga-DOTANOC and ^{68}Ga-DOTATATE using a randomized crossover design. Labeling of DOTANOC and DOTATATE with ^{68}Ga was standardized using a fully automated synthesis device. PET/CT findings were compared with 3-phase CT scans and in some patients with MR imaging, ^{18}F-FDG PET/CT, and histology. Uptake in organs and tumor lesions was quantified and compared by calculation of maximum standardized uptake values (SUVmax) using volume computer-assisted reading. **Results:** Histology revealed low-grade GEP-NETs (G1) in 4 patients, intermediate grade (G2) in 7, and high grade (G3) in 7. ^{68}Ga-DOTANOC and ^{68}Ga-DOTATATE were false-negative in only 1 of 18 patients. In total, 248 lesions were confirmed by cross-sectional and PET imaging. The lesion-based sensitivity of ^{68}Ga-DOTANOC PET was 93.5%, compared with 85.5% for ^{68}Ga-DOTATATE PET ($P = 0.005$). The better performance of ^{68}Ga-DOTANOC PET is attributed mainly to the significantly higher detection rate of liver metastases rather than tumor differentiation grade. Multivariate analysis revealed significantly higher SUVmax in G1 tumors than in G3 tumors ($P = 0.009$). This finding was less pronounced with ^{68}Ga-DOTANOC ($P > 0.001$). Altogether, ^{68}Ga-DOTANOC changed treatment in 3 of 18 patients (17%). **Conclusion:** The $sst_{2,3,5}$-specific radiotracer ^{68}Ga-DOTANOC detected significantly more lesions than the sst_2-specific radiotracer ^{68}Ga-DOTATATE in our patients with GEP-NETs. The clinical relevance of this finding has to be proven in larger studies.

Key Words: neuroendocrine tumors; ^{68}Ga; PET/CT; somatostatin receptor targeting; DOTA-NOC

J Nucl Med 2013; 54:364–372
DOI: 10.2967/jnumed.112.111724

Gastroenteropancreatic neuroendocrine tumors (GEP-NETs) are a heterogeneous group of tumors that originate from the diffuse neuroendocrine system of the gastrointestinal tract or bronchopulmonary system. They are characterized by the overexpression of somatostatin receptors. To date, 5 somatostatin receptor subtypes (sst_1–sst_5) have been identified, all of which are expressed with differing frequencies in GEP-NETs. For example, sst_2 and sst_5 are expressed at a high density in 70%–100% of GEP-NETs (*1*). These receptors have been used as a target for diagnostic and therapeutic radiotracers. [^{111}In-diethylenetriaminepentaacetic acid (DTPA)]-octreotide, an sst_2-specific tracer, was the first radiolabeled somatostatin analog to become an integral part of the routine diagnostic work-up of patients with GEP-NETs (*2*). ^{90}Y- and ^{177}Lu-labeled DOTA-conjugated sst_2 tracers such as ^{90}Y-DOTATOC ([^{90}Y-DOTA, Tyr^3]-octreotide) and ^{177}Lu-DOTATATE ([^{177}Lu-DOTA,Tyr^3]-octreotate) are being successfully introduced in peptide receptor radionuclide therapy (*3,4*).

Most clinically used radiolabeled somatostatin analogs are agonists, which bind with high affinity only to sst_2. Although most NETs express sst_2, the distribution and density of sst_2 is often variable and sometimes too low for effective somatostatin receptor targeting (*1*). This is likely the reason for the wide sensitivity range (60%–100%) of

Received Jul. 23, 2012; revision accepted Sep. 25, 2012.
For correspondence contact: Damian Wild, Division of Nuclear Medicine, University Basel Hospital, Petersgraben 4, CH-4031 Basel, Switzerland.
E-mail: dwild@uhbs.ch
Published online Jan. 7, 2013.

^{111}In-DTPA-octreotide scintigraphy and SPECT in the detection of NETs (*5*). One possible approach to overcoming this problem is the use of radiolabeled tracers with affinity to more than one somatostatin receptor subtype. Gastrinomas, ileal carcinoids, and VIPomas express sst_2 or sst_5 with an incidence of almost 100% (*1*). [DOTA, 1-Nal^3]-octreotide (DOTANOC) is a peptide that promises to target a broader range of somatostatin subtype receptors, including sst_2, sst_3, and sst_5 (*6,7*). Preliminary results in single patients suggest that this new radiopeptide locates more metastases than do sst_2-specific tracers (*7,8*). This finding is supported by Asnacios et al., who found sst_3 and sst_5 expression in ^{111}In-DTPA-octreotide–negative tumors (*9*).

Furthermore, ^{68}Ga-based radiopharmaceuticals such as ^{68}Ga-DOTANOC showed higher binding affinities to sst_2 and sst_5 than do the respective lutetium and indium derivatives. The higher binding affinity resulted in significantly higher tumor uptake in a tumor-bearing rat model (*8*). This finding is relevant because metallic ^{68}Ga is a positron emitter with a half-life of 68 min that is ideal for molecular PET imaging. Recently, somatostatin receptor PET using ^{68}Ga-DOTATOC or ^{68}Ga-DOTATATE showed promising results in patients, with a higher lesion detection rate than was achieved with ^{111}In-DTPA-octreotide scintigraphy and SPECT (*10–12*). But more important, somatostatin receptor PET changed the clinical management in most patients with negative or inconclusive findings on ^{111}In-DTPA-octreotide scintigraphy (*12*). Currently, ^{68}Ga-DOTATOC, ^{68}Ga-DOTATATE, and ^{68}Ga-DOTANOC are the most established somatostatin receptor PET tracers (*13*). Comparison of ^{68}Ga-DOTATOC and ^{68}Ga-DOTATATE (both sst_2-specific tracers) in the same patient revealed comparable diagnostic accuracy for the detection of NET lesions (*14*). Another study compared the tumor detection rates between ^{68}Ga-DOTATATE PET (sst_2-specific PET) and ^{68}Ga-DOTANOC PET ($sst_{2,3,5}$-specific PET) in the same patient (*15*).

Our study had 3 aims: first, to perform a prospective patient- and lesion-based comparison of ^{68}Ga-DOTATATE and ^{68}Ga-DOTANOC PET in the same patient; second, to establish whether there is any correlation between tumor grade and lesion identification using ^{68}Ga-DOTATATE and ^{68}Ga-DOTANOC PET; and finally, to evaluate whether ^{68}Ga-DOTANOC PET/CT alters clinical management in patients with negative ^{68}Ga-DOTATATE PET/CT findings.

MATERIALS AND METHODS

Patients and Study Design

This prospective single-center study compared ^{68}Ga-DOTATATE and ^{68}Ga-DOTANOC PET/CT in the same patient using a crossover design in random order. All recruited patients were under prospective follow-up at the Neuroendocrine Tumor Unit, Royal Free Hospital, London. Inclusion criteria were age 25–85 y, biopsy-proven metastatic GEP-NET (G1–G3), and an indication for staging or restaging imaging including CT scanning or MR imaging as part of the patients' general surveillance. Exclusion criteria were known disseminated disease, pregnancy, kidney insufficiency (creatinine level $>$ 1.5 mg/dL), treatment with short-acting somatostatin analogs less than 3 d before somatostatin receptor PET, and octreotide depot injection less than 4 wk before somatostatin receptor PET. All patients underwent sst_2 and $sst_{2,3,5}$ PET/CT (^{68}Ga-DOTATATE and ^{68}Ga-DOTANOC PET/CT) at the University College London Hospital.

The study was approved by the local institutional review board, and written informed consent was obtained in accordance with provisions of the Declaration of Helsinki.

Synthesis and Radiolabeling of DOTATATE and DOTANOC

The peptide–chelator conjugates [DOTA,Tyr^3]-octreotate (DOTATATE) and [DOTA,1-Nal^3]-octreotide (DOTANOC) were synthesized by standard Fmoc solid-phase synthesis on 2-chlorotritylchloride resin on a peptide synthesizer (Switch 24; Rink CombiChem Technologies), according to a general procedure described previously (*6*). ^{68}Ga-DOTATATE and ^{68}Ga-DOTANOC were labeled under sterile conditions in an isolator using a modification of the method described by Zhernosekov et al. (*16*) and Shastry et al. (*17*). Briefly, a TiO_2-based commercially available ^{68}Ge–^{68}Ga generator (Eckert and Ziegler) was eluted with 0.1N hydrochloric acid. Chemical purification and volume concentration of ^{68}Ga was performed in an 80% acetone/0.15N HCl solution using a cation exchange resin (400-mesh AG 50W-X8 resins; Bio-Rad). Afterward, about 60 μg of DOTATATE or DOTANOC were incubated with 600–1,200 MBq of ^{68}Ga at 90°C for 10 min (pH, ~3.5). For further purification, the reaction solution was passed over a C_{18} cartridge (Sep-Pak; Waters), washed with 3 mL of saline, and eluted with 1 mL of 50% ethanol. The final product was diluted with 7 mL of saline and then subjected to sterile filtration using a Millex 0.22-μm filter (Millipore). The labeling yield was analyzed by silica gel instant thin-layer chromatography (Pall Inc.) and by high-performance liquid chromatography using a Luna 5-μm, C18 (2) 50 × 3.0-mm column (Phenomenex) and an acetonitrile–water gradient. The labeling yield and radiochemical purity of ^{68}Ga-DOTATATE and ^{68}Ga-DOTANOC were greater than 98% at a specific activity of 14.5–34 GBq/μmol.

Imaging

^{68}Ga-DOTATATE and ^{68}Ga-DOTANOC PET/CT scans were obtained within 6–48 h of each other in all patients except patient 2, who had 27 d between scans. Images were acquired 54–73 min after injection of 155 ± 17 MBq (mean ± SD) (range, 135–170 MBq) of ^{68}Ga-DOTATATE and 60–74 min after injection of 155 ± 12 MBq (130–170 MBq) of ^{68}Ga-DOTANOC. The administered mass of ^{68}Ga-DOTATATE and ^{68}Ga-DOTANOC was 28 ± 7 μg (17–43 μg) and 33 ± 7 μg (21–45 μg) ($P > 0.08$), respectively. All patients were scanned with the same dedicated PET/CT unit (Discovery ST 16; GE Healthcare) from the vertex to the mid thigh.

The CT exposure factors for all examinations were 140 kVp and 80–120 mAs. PET acquisition was performed in 3 dimensions with 4 min per bed position and a 5-slice overlap. PET images were reconstructed using an ordered-subsets expectation maximization (OSEM) algorithm with 3 iterations and 25 subsets and with CT-based attenuation correction.

The presence of lesions was confirmed by 3-phase, thin-section multidetector CT or gadolinium-enhanced MR imaging. In all

patients with poorly differentiated neuroendocrine carcinoma (G3), additional ^{18}F-FDG PET/CT scans were obtained using a dedicated PET/CT unit (Discovery ST 16; GE Healthcare) and a standard protocol (*18*). All scans were performed within 6 wk of one another.

Diagnostic (3-phase) CT scans were obtained on a Brilliance 64-slice scanner (Phillips Medical System) or a Lightspeed scanner (GE Healthcare). All scans were acquired at 120 kVp and variable amperage, depending on body habitus. The scans were reconstructed at 3-mm (Brilliance) or 5-mm (Lightspeed) intervals. Intravenous contrast material (Omnipaque 300; GE Healthcare) was administered via a pump injector (E-Z-EM) at 3.5 mL/s.

The MR scanner was a 1.5-T Achieva (Phillips Medical Systems). All scans were acquired using the Synergy Sense body coil. Contrast material (Dotarem; Guerbet) was administered via a cannula in an antecubital vein using a pump injector (Medrad) at 1.5 mL/s with a 20-mL saline flush.

Image Analysis

Two experienced dedicated nuclear medicine physicians independently assessed the ^{68}Ga-DOTATATE and ^{68}Ga-DOTANOC PET/CT scans. The physicians were unaware of the patients' identities, type of scan, or results of other imaging modalities. The number of lesions that could be identified clearly as a single focus was determined for each patient. To enable a methodic and consistent approach to the identification of lesions, 4 categories of lesion sites were specified: lymph nodes, liver, bone, and other locations. Afterward, ^{68}Ga-DOTATATE and ^{68}Ga-DOTANOC PET/CT scans were compared in both a patient-by-patient and a lesion-by-lesion analysis. A dual-accredited radiologist/nuclear medicine physician compared areas of abnormal tracer uptake with CT, MR imaging, and ^{18}F-FDG PET/CT to confirm the presence of lesions.

^{68}Ga-DOTATATE and ^{68}Ga-DOTANOC organ and tumor uptake was quantified using maximum standardized uptake values (SUVmax). Organ uptake was measured by drawing regions of interest over 3 consecutive transaxial PET slices, whereas tumor uptake was determined using PET VCAR (volume computer-assisted reading) software (GE Healthcare).

Statistical Analysis

The sensitivity and 95% confidence interval of both imaging modalities were calculated according to the method of Blaker et al. (*19*). The statistical significance of the difference in sensitivity between the 2 tracers was analyzed by testing for equality of proportions (*20*).

The organ update was compared using the Wilcoxon matched-pairs signed-rank test.

Linear mixed-effects models were used to describe the association between SUVmax (and tumor-to-background activity ratio [TBR]) and multiple explanatory variables by treating them as fixed effects. To properly reflect the structure of the repeated data, patient number and lesion number nested within patient were treated as random effects. The model was adapted to reflect the crossover design of the study (i.e., paired ^{68}Ga-DOTATATE and ^{68}Ga-DOTANOC measures per lesion). Ki-67 index, type of tracer, and location of the lesion were used as explanatory variables. Only significant interactions were included in the final model. All continuous variables were log-transformed and centered on the mean (response variables were not centered). The residuals of model fits were repeatedly visually inspected for violations of model assumptions, and the Akaike information criterion was used for model selection.

RESULTS

From 21 consecutive enrolled patients, 3 patients were excluded from analysis due to disseminated disease (1 patient) or insufficient comparison with morphologic imaging (2 patients). The remaining 18 patients (8 women and 10 men; mean age ± SD, 58 ± 12 y) were eligible for inclusion in this study. Patient characteristics are summarized in Table 1.

Both ^{68}Ga-DOTATATE PET and ^{68}Ga-DOTANOC PET revealed disease in 17 of 18 patients (94.4%; 95% confidence interval, 73.4%–99.7%). In 1 patient neither tracer was able to identify the tumor, and this patient had a histologically confirmed high-grade hindgut neuroendocrine tumor.

None of the patients experienced any subjective symptoms after the injection of either radiotracer.

Lesion Analysis

In total, 248 lesions were confirmed by cross-sectional and PET imaging (Table 2) ^{68}Ga-DOTANOC PET and ^{68}Ga-DOTATATE PET detected 232 and 212 lesions, respectively. CT was performed on all patients, MR imaging on 7 of 18 patients, and ^{18}F-FDG PET on all patients with G3 GEP-NETs. The overall sensitivity of ^{68}Ga-DOTANOC PET was 93.5% (95% confidence interval, 89.4%–96.1%), compared with 85.5% (95% confidence interval, 80.6%–89.9%) for ^{68}Ga-DOTATATE PET ($P = 0.005$). This difference is attributed mainly to the significantly higher detection rate of liver metastases with ^{68}Ga-DOTANOC PET (Figs. 1–3) ($P < 0.001$). In patient 2, for example, ^{68}Ga-DOTANOC PET detected all 3 liver metastases whereas ^{68}Ga-DOTATATE PET detected only 1 liver metastasis (Figs. 1 and 2). Slightly more bone lesions were detected with ^{68}Ga-DOTATATE PET (Table 2). Neither ^{68}Ga-DOTANOC PET nor ^{68}Ga-DOTATATE PET showed significant advantages in the detection of lesions in the remaining organs, including lymph nodes. However, ^{68}Ga-DOTANOC PET detected 7 of 8 pancreatic NETs whereas ^{68}Ga-DOTATATE PET detected only 3 of 8 pancreatic NETs. In patients 2 and 7, both tracers detected a pancreatic lesion (uncinate process) that was not confirmed by cross-sectional and follow-up imaging.

The tumor grade of all patients was determined histologically using mitotic rates and Ki-67 indices (European Neuroendocrine Tumor Society proposal for grading GEP-NETs) (*21*): 4 patients had low-grade (G1), 7 intermediate-grade (G2), and 7 high-grade (G3) GEP-NETs. The higher sensitivity of ^{68}Ga-DOTANOC PET in patients with G1 GEP-NETs can be explained by the larger portion of liver lesions in this subgroup (Table 2).

Among the 18 patients, management was altered in 3 patients (patients 8, 10, and 12) after ^{68}Ga-DOTANOC

TABLE 1
Characteristics of Study Population

Patient no.	Age (y)	Sex	Tumor location	Tumor grade*	Tumor growth fraction† (%)	Indication
1	64	F	Hindgut NET	G3	70	Restaging
2	37	M	Pancreatic NET	G3	30	Restaging
3	73	M	Midgut NET	G2	3	Restaging
4	62	M	Pancreatic NET	G1	1	Restaging
5	59	M	Midgut NET	G2	5	Restaging
6	51	M	Midgut NET	G1	<1	Staging
7	65	F	Midgut NET	G2	15	Restaging
8	69	F	Hindgut NET	G2	15	Restaging
9	63	M	Unknown primary	G3	50	Staging
10	67	F	Pancreatic NET	G1	<2	Staging
11	57	F	Pancreatic NET	G2	5	Restaging
12	44	M	Pancreatic NET	G3	>20	Restaging
13	71	M	Hindgut NET	G3	90	Staging
14	41	M	Pancreatic NET	G2	15	Staging
15	80	F	Midgut NET	G3	40	Staging
16	46	F	Midgut NET	G1	<2	Staging
17	56	M	Foregut NET	G2	<20	Restaging
18	54	F	Pancreatic NET	G3	33	Restaging

*According to European Neuroendocrine Tumor Society proposal for grading GEP-NETs (*21*).
†Ki-67 index was used to determine tumor growth fraction.

PET/CT. These patients had more extensive surgery than initially planned because ^{68}Ga-DOTANOC PET/CT revealed more extensive disease than ^{68}Ga-DOTATATE PET/CT and morphologic imaging.

Tumor and Organ Uptake

SUVmax was available for 104 lesions. Table 3 shows the median SUVmax for ^{68}Ga-DOTANOC and ^{68}Ga-DOTATATE, together with the interquartile range. Overall, there was higher tumor uptake of ^{68}Ga-DOTATATE than of ^{68}Ga-DOTANOC (Table 3). However, in some patients (patients 2, 9, 10, 11, 12, 14, 15, and 20) median tumor SUVmax was higher for ^{68}Ga-DOTANOC (Figs. 1–3). The tumor uptake of both tracers was highly organ-specific (Table 3). The highest tumor uptake was found in the liver, and the lowest tumor uptake was found in the bone.

Importantly, the tumor uptake of ^{68}Ga-DOTATATE and ^{68}Ga-DOTANOC was dependent on tumor grade. Table 3 shows that the median SUVmax decreased as the tumor grade increased. Multivariate analysis using a mixed-effects model with the categoric variable tumor grade (G1–G3) revealed a significantly higher SUVmax in low-grade (G1) than in-high grade (G3) tumors ($P = 0.009$). This finding was less pronounced with ^{68}Ga-DOTANOC ($P = 0.003$). ^{68}Ga-DOTATATE showed significantly higher uptake than did ^{68}Ga-DOTANOC in G1 and G2 tumors but not in G3 tumors.

TABLE 2
Lesion-Based Comparison of ^{68}Ga-DOTATATE PET, ^{68}Ga-DOTANOC PET, and Conventional Imaging (CT, MR Imaging, or ^{18}F-FDG PET/CT)

Tumor location/tumor type	Patients*	^{68}Ga-DOTATATE lesions	^{68}Ga-DOTANOC lesions	P†	CT, MR imaging, ^{18}F-FDG PET/CT
Liver	13	68	88	<0.001	93
Lymph nodes	7	39	42	0.36	43
Bone	10	89	82	0.02	89
Other organs	14	16	20	0.28	23
Total	18	212	232	0.005	248
G1 GEP-NET	4	43	51	0.02	52
G2 GEP-NET	7	78	81	0.53	85
G3 GEP-NET	7	91	100	0.12	111
Total	18	212	232	0.005	248

*Number of patients in whom lesion analysis was available.
†^{68}Ga-DOTATATE and ^{68}Ga-DOTANOC were compared in lesion-by-lesion analysis using multivariate mixed-effects model.

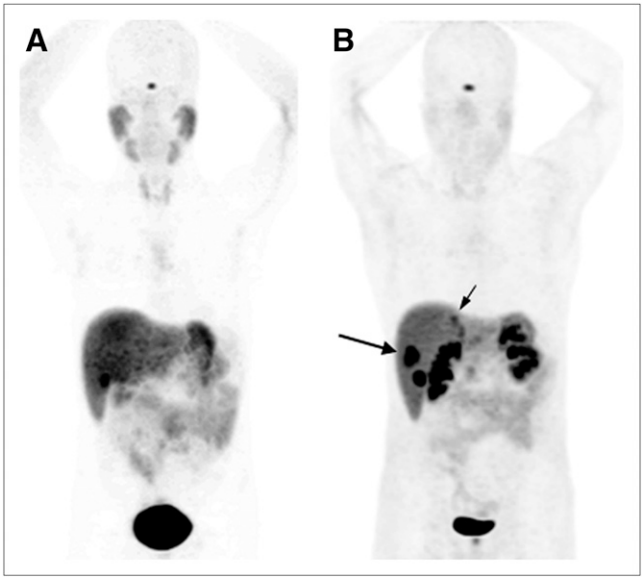

FIGURE 1. ^{68}Ga-DOTATATE (A) and ^{68}Ga-DOTANOC (B) whole-body PET scans from patient 2. Both scans were performed within 27 d of each other. There are 3 focal ^{68}Ga-DOTANOC–avid lesions in right liver lobe (B), whereas ^{68}Ga-DOTATATE shows only 1 liver lesion (A). Arrows show lesions that were only ^{68}Ga-DOTANOC–avid.

Quantification of tracer uptake in organs revealed significantly higher uptake of ^{68}Ga-DOTATATE in all relevant organs except the pituitary and bone marrow (Table 4). In the bone marrow, ^{68}Ga-DOTANOC showed significantly higher uptake than did ^{68}Ga-DOTATATE ($P < 0.001$). In the pituitary, however, no significant difference was found between the tracers. Organ uptake was not dependent on tumor grade.

An important characteristic of a successful imaging probe is a high TBR. ^{68}Ga-DOTANOC showed a significantly higher TBR in lesions of the liver, whereas ^{68}Ga-DOTATATE showed a significantly higher TBR in lesions of the bone (Table 5). TBRs for both tracers were significantly lower in the liver than in any other organs ($P < 0.001$). The grade of differentiation did not have a significant effect on the TBR of the 2 tracers.

DISCUSSION

Somatostatin receptor PET has shown promising results in NETs, with a higher lesion detection rate than is achieved with ^{18}F-fluorodihydroxyphenyl-L-alanine PET, somatostatin receptor SPECT, CT, or MR imaging (*10, 11,22,23*). Currently, ^{68}Ga-DOTATOC, ^{68}Ga-DOTATATE, and ^{68}Ga-DOTANOC are the most established somatostatin receptor PET tracers (*13*). Comparison studies by Poeppel et al. (*14*) (comparison of ^{68}Ga-DOTATATE and ^{68}Ga-DOTATOC) and Kabasakal et al. (*15*) (comparison of ^{68}Ga-DOTATATE and ^{68}Ga-DOTANOC) showed a similar diagnostic accuracy for these tracers for the detection of NETs. In our study, we prospectively compared ^{68}Ga-DOTATATE PET/CT and ^{68}Ga-DOTANOC PET/CT in the same patient. In contrast to the findings of Kabasakal et al. (*15*), we detected significantly more lesions with ^{68}Ga-DOTANOC PET (sensitivity, 93.5%) than with ^{68}Ga-DOTATATE PET (sensitivity, 85.5%). The better performance of ^{68}Ga-DOTANOC PET is attributed mainly to the significantly higher detection rate of liver metastases.

There are 2 possible explanations for this finding. First, normal liver uptake of ^{68}Ga-DOTANOC is significantly lower than that of ^{68}Ga-DOTATATE, resulting in a significantly higher TBR and tumor detection rate for ^{68}Ga-DOTANOC than for ^{68}Ga-DOTATATE. This finding is a surprise, as the more lipophilic radiotracer ^{68}Ga-DOTANOC is expected to show higher liver uptake. However, the C-terminal carboxylate group of DOTATATE may be responsible for some of the anion transport mechanism of ^{68}Ga-DOTATATE into human liver cells (*24*).

The broader somatostatin receptor binding profile of ^{68}Ga-DOTANOC might be another explanation for the better performance of ^{68}Ga-DOTANOC in the detection of liver metastases. This assumption is supported by tumor

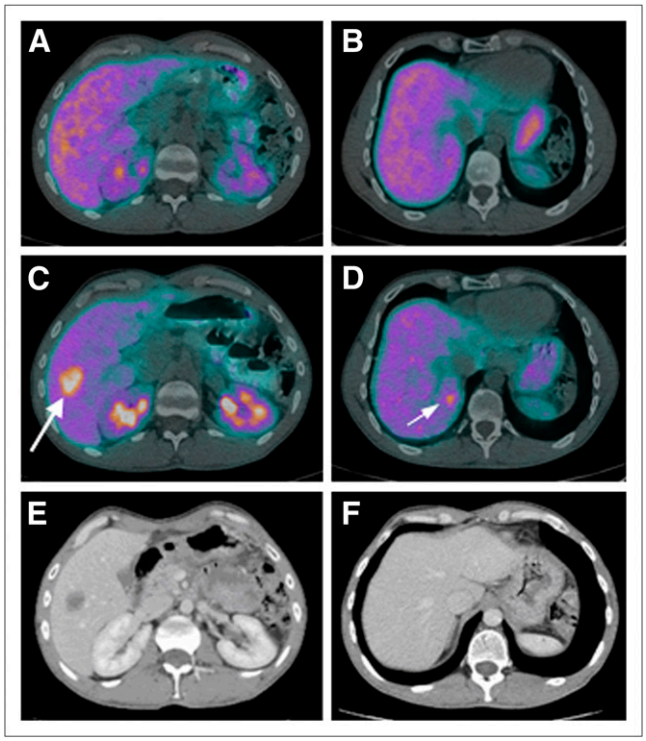

FIGURE 2. ^{68}Ga-DOTATATE (A and B) and ^{68}Ga-DOTANOC (C and D) PET/CT scans and contrast-enhanced CT scans (E and F) from patient 2 (addendum to Fig. 1). Both PET/CT scans were obtained within 27 d of each other. Large arrow shows focal ^{68}Ga-DOTANOC uptake in hypodense liver lesion (E) that is not ^{68}Ga-DOTATATE–avid (A). There is subtle but definite ^{68}Ga-DOTANOC uptake in liver segment 7 (small arrow) without ^{68}Ga-DOTATATE and CT correlation (B and F, respectively). In this patient, right hemihepatectomy was performed as curative attempt. Histology confirmed ^{68}Ga-DOTANOC PET/CT findings.

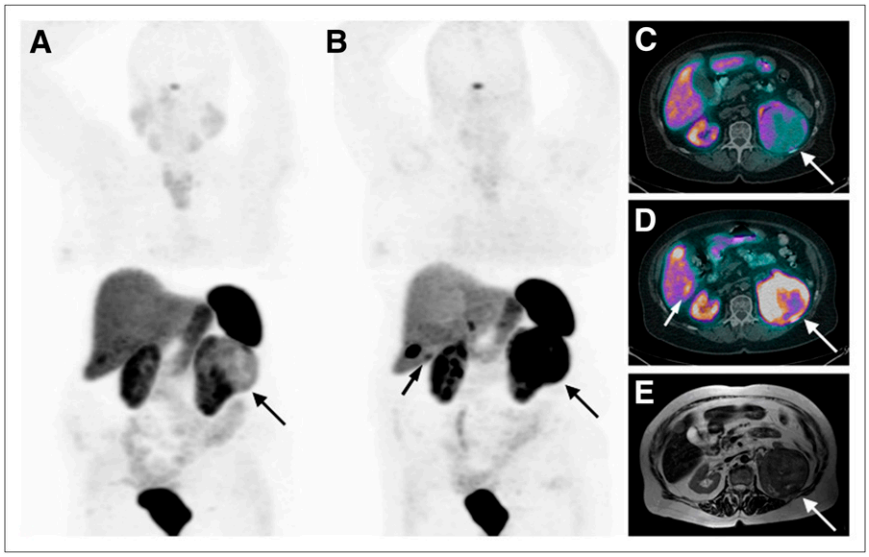

FIGURE 3. ^{68}Ga-DOTATATE (A) and ^{68}Ga-DOTANOC (B) whole-body PET scans, ^{68}Ga-DOTATATE (C) and ^{68}Ga-DOTANOC (D) PET/CT scans, and T2-weighted MR scan from patient 8. Both PET/CT scans were obtained within 48 h of each other. Small arrow shows subtle but definite ^{68}Ga-DOTANOC uptake (B and D) in segment 6, without MR imaging or ^{68}Ga-DOTATATE correlation (A, C, and E). Large kidney metastasis (large arrow) shows higher uptake of ^{68}Ga-DOTANOC than of ^{68}Ga-DOTATATE, with SUVmax of 20.9, compared with 12.3. In this patient, left kidney resection and segmentectomy of liver (segments 5 and 6) were performed as curative attempt. Histology confirmed ^{68}Ga-DOTANOC PET/CT findings.

uptake studies. ^{68}Ga-DOTANOC, which binds specifically to sst_2, sst_3, and sst_5 (*7*), showed higher tumor uptake in 14 of 39 liver metastases despite having a 10 times lower sst_2 affinity than the sst_2-specific tracer ^{68}Ga-DOTATATE (*8*). Thus, $sst_{3,5}$-mediated accumulation of ^{68}Ga-DOTANOC might be the reason for the higher ^{68}Ga-DOTANOC uptake in about one third of liver metastases.

^{68}Ga-DOTATATE shows significantly higher uptake in all organs with predominant sst_2 expression (*25–32*). However, intense ^{68}Ga-DOTANOC uptake is found in the pituitary, which is the only organ that shows consistently high sst_2 and sst_5 expression (*25,33,34*). Again, sst_5-mediated accumulation of ^{68}Ga-DOTANOC might be the explanation for this finding.

We have reviewed the somatostatin receptor expression of different normal organs to the best of our knowledge. However, this is a difficult task because sst_1–sst_5 in vitro detection has been studied with distinctly different methods (polymerase chain reaction [PCR], immunohistochemistry, autoradiography) with often contradictory results (*25–34*).

The significantly lower uptake of ^{68}Ga-DOTANOC in normal pancreas tissue is likely responsible for the higher tumor detection rate in the pancreas (7 tumors), compared with that for ^{68}Ga-DOTATATE (3 tumors). In 2 patients with multiple endocrine neoplasia type 1, ^{68}Ga-DOTATATE detected only one pancreatic tumor whereas ^{68}Ga-DOTANOC detected multiple pancreatic tumors. This finding was clinically relevant because the treatment was altered in both patients, who underwent more extensive surgery. Altogether, ^{68}Ga-DOTANOC changed treatment in 3 of 18 patients (17%). Both tracers showed false-positive results in the pancreas (uncinate process) of 2 patients. This false-positive finding has been described before (*35*). There was 1 further false-positive result with ^{68}Ga-DOTATATE in the

TABLE 3
Median Tumor Uptake (SUVmax) and Interquartile Range of ^{68}Ga-DOTATATE and ^{68}Ga-DOTANOC

		^{68}Ga-DOTATATE		^{68}Ga-DOTANOC		
Tumor location/tumor type	Number of lesions*	SUVmax	Interquartile range	SUVmax	Interquartile range	$P^{\dagger}$
Liver	39	14.5	11.8–21.7	13.8	9.0–21.1	0.25
Lymph nodes	20	10.4	4.1–23.3	8.7	4.2–22.5	0.30
Bone	22	6.3	4.1–13.9	6.2	2.6–10.5	<0.001
Other organs	23	12.3	4.9–17.2	7.2	5.2–18.9	0.80
Total	104	12.4	6.3–20.8	9.2	5.8–20.0	
G1 GEP-NET	33	22.6	13.1–30.8	21.9	7.5–26.8	0.007
G2 GEP-NET	49	14.2	8.4–20.4	10.3	6.0–17.0	<0.001
G3 GEP-NET	22	8.3	3.7–12.3	7.2	4.1–13.5	0.12
Total	104	12.4	6.3–20.8	9.2	5.8–20.0	

*Number of patients in whom lesion analysis was available.

†^{68}Ga-DOTATATE and ^{68}Ga-DOTANOC tumor uptake, measured by SUVmax, was compared using multivariate mixed-effects model. Same statistical model was used for comparison of tumor uptake in different organs: $P_{lymph:liver} = 0.046$, $P_{bone:liver} = 0.012$, $P_{other\ organs:liver} = 0.004$, $P_{intermediate:low} = 0.073$, $P_{high:low} = 0.009$.

TABLE 4
Median Organ Uptake (SUVmax) and Interquartile Range of ^{68}Ga-DOTATATE and ^{68}Ga-DOTANOC

Organ	sst expression*	Reference*	^{68}Ga-DOTATATE SUVmax	^{68}Ga-DOTATATE Interquartile range	^{68}Ga-DOTANOC SUVmax	^{68}Ga-DOTANOC Interquartile range	P†
Pituitary	$sst_2 = sst_5 > sst_{1,3} > sst_4$	*25,33,34*	6.1	5.2–7.0	6.6	5.6–7.7	0.41
Adrenals	$sst_2 = sst_1 > sst_{4,5} > sst_3$	*25–28*	10.1	8.8–13.6	8.9	7.4–10.7	0.003
Pancreas	$sst_2 > sst_{1,3,5}$	*25,29,30*	3.5	3.0–4.3	2.5	2.0–3.4	<0.001
Stomach	$sst_2 > sst_1$	*25,31*	10.1	8.2–13.9	5.7	4.4–7.2	<0.001
Spleen	sst_2	*25,32*	28.2	20.9–31.2	24.1	14.2–27.7	0.02
Thyroid	$sst_2 > sst_1$	*25*	2.4	1.8–3.4	1.6	1.3–2.2	0.001
Parotid gland	sst_2	*25*	2.5	2.2–4.1	0.9	1.3–1.6	<0.001
Liver	sst_1	*25*	7.5	5.6–9.8	5.1	4.1–5.8	<0.001
Bone marrow	Not done	Not done	0.6	0.5–0.8	1.3	1.0–1.5	<0.001

*Somatostatin receptor subtype expression with corresponding reference.
†^{68}Ga-DOTATATE and ^{68}Ga-DOTANOC organ uptake, measured by SUVmax, was compared using Wilcoxon paired signed rank test.

prostate. The false-positive findings were confirmed by more than 1 y of follow-up, morphologic imaging (MR imaging), and biopsy of the prostate.

In contrast to liver metastases and pancreatic tumors, bone metastases were significantly more frequently detected by ^{68}Ga-DOTATATE PET than by ^{68}Ga-DOTANOC PET. This difference can be explained by the lower background activity (bone marrow activity) of ^{68}Ga-DOTATATE, resulting in a significantly higher TBR. Unfortunately the mechanism of ^{68}Ga-DOTATATE and ^{68}Ga-DOTANOC accumulation in the bone marrow is not known. Therefore, no assumption can be made as to whether somatostatin receptor expression is responsible for the difference in bone marrow uptake between the 2 radiotracers. There was no difference in the tumor detection rate between the 2 tracers in lymph nodes or any other organs.

Comparison of tumor grade and detection rate showed that ^{68}Ga-DOTANOC detected significantly more lesions than did ^{68}Ga-DOTATATE in patients with G1 GEP-NETs. This difference can be explained by the larger proportion of liver lesions in this patient subgroup. There was no significant difference between the 2 tracers in the tumor detection rate of G2 and G3 tumors. Within the literature, there is evidence that somatostatin receptor PET is of limited value in patients with G3 NETs and that ^{18}F-FDG PET may be more suitable in these cases (*18*). In our study, however, ^{68}Ga-DOTATATE and ^{68}Ga-DOTANOC PET detected significantly more G3 lesions (82% and 90%, respectively) than did ^{18}F-FDG PET (58%). Importantly, tumor uptake of ^{68}Ga-DOTATATE and ^{68}Ga-DOTANOC was dependent on tumor grade. The median tumor SUVmax decreased as the tumor grade increased. This finding can be explained by the loss of somatostatin receptors during the process of tumor dedifferentiation.

To our knowledge, only our group and Kabasakal et al. (*15*) compared ^{68}Ga-DOTATATE and ^{68}Ga-DOTANOC

TABLE 5
Median TBR and Interquartile Range for ^{68}Ga-DOTATATE and ^{68}Ga-DOTANOC

Tumor location/tumor type	Number of lesions*	^{68}Ga-DOTATATE TBR	^{68}Ga-DOTATATE Interquartile range	^{68}Ga-DOTANOC TBR	^{68}Ga-DOTANOC Interquartile range	P†
Liver	39	2.0	1.4–2.7	2.7	1.8–3.7	<0.001
Lymph nodes	20	7.7	4.9–13.3	6.1	3.5–13.9	0.26
Bone	22	10.4	6.3–15.7	8.8	3.8–14.5	<0.001
Other organs	23	4.8	2.4–11.4	6.3	4.0–10.8	0.36
Total	104	3.8	2.2–9.9	4.2	2.7–9.0	
G1 GEP-NET	33	5.0	2.0–10.5	6.0	2.9–10.4	0.37
G2 GEP-NET	49	3.0	1.8–6.3	3.1	2.0–4.6	0.27
G3 GEP-NET	22	4.8	2.5–18.0	6.2	4.5–16.7	0.068
Total	104	3.8	2.2–9.9	4.2	2.7–9.0	

*Number of lesions for which TBR values were available.
†TBR values of ^{68}Ga-DOTATATE and ^{68}Ga-DOTANOC were compared using multivariate mixed-effects model. Same statistical model was used for comparison of TBR values in different organs: $P_{lymph:liver} < 0.001$, $P_{bone:liver} < 0.001$, $P_{other\ organs:liver} < 0.001$, $P_{intermediate:low} = 0.08$, $P_{high:low} = 0.22$.

PET/CT in the same patient. Several factors may explain the difference between our findings and those of Kabasakal. First, the studied patient populations were relatively small, with overlapping confidence intervals for sensitivity. A higher bone-to-liver lesion ratio in the study of Kabasakal et al. might additionally explain the better performance of ^{68}Ga-DOTATATE in their study than in ours. Furthermore, their Figure 3 (patient 5) attracts some attention because the pituitary shows almost no uptake of ^{68}Ga-DOTANOC—in contrast to their Figure 1 (*15*) and our data. Importantly, we always found high uptake of ^{68}Ga-DOTANOC in the pituitary. The minimal uptake of ^{68}Ga-DOTANOC in the pituitary in their study indicates either a quality problem with the radiotracer (*36*) or possible saturation of sst receptors, which may influence the performance of the tracer and explain the discordant results compared with our study.

The most relevant limitation of this study was the lack of pathologic confirmation of most lesions (238/248 lesions). For ethical and practical reasons, it was not possible to obtain histologic verification of all lesions. However, in all patients who had surgery, ^{68}Ga-DOTANOC findings were histologically confirmed (4/18 patients). Furthermore, the presence of lesions was confirmed by CT and, where indicated, by MR imaging and ^{18}F-FDG PET/CT. The combination of CT, MR imaging, and ^{18}F-FDG PET/CT detected more lesions than ^{68}Ga-DOTANOC or ^{68}Ga-DOTATATE PET.

CONCLUSION

The $sst_{2,3,5}$-specific radiotracer ^{68}Ga-DOTANOC detected significantly more lesions than did the sst_2-specific radiotracer ^{68}Ga-DOTATATE in our patients with GEP-NETs. Because of the small size of our study population, additional, larger, trials are needed to confirm whether our results are of clinical relevance and would justify the widespread adoption of ^{68}Ga-DOTANOC over ^{68}Ga-DOTATATE.

DISCLOSURE

The costs of publication of this article were defrayed in part by the payment of page charges. Therefore, and solely to indicate this fact, this article is hereby marked "advertisement" in accordance with 18 USC section 1734. This work was supported in part by the Swiss National Science Foundation (grant PASMP3-123269), the Novartis Foundation, the Department of Health's NIHR Biomedical Research Centre's funding scheme, and the King's College London and UCL Comprehensive Cancer Imaging Centre CR-U.K. and EPSRC, in association with the MRC and DoH (England). No other potential conflict of interest relevant to this article was reported.

ACKNOWLEDGMENT

We thank Irfan Kayani for assistance in interpreting CT and MR imaging results.

REFERENCES

1. Reubi JC, Waser B. Concomitant expression of several peptide receptors in neuroendocrine tumours: molecular basis for in vivo multireceptor tumour targeting. *Eur J Nucl Med Mol Imaging.* 2003;30:781–793.
2. Kwekkeboom DJ, Krenning EP, Scheidhauer K, et al. ENETS Consensus Guidelines for the Standards of Care in Neuroendocrine Tumors: somatostatin receptor imaging with ^{111}In-pentetreotide. *Neuroendocrinology.* 2009;90: 184–189.
3. Kwekkeboom DJ, de Herder WW, Kam BL, et al. Treatment with the radiolabeled somatostatin analog [177 Lu-DOTA 0,Tyr3]octreotate: toxicity, efficacy, and survival. *J Clin Oncol.* 2008;26:2124–2130.
4. Imhof A, Brunner P, Marincek N, et al. Response, survival, and long-term toxicity after therapy with the radiolabeled somatostatin analogue [^{90}Y-DOTA]-TOC in metastasized neuroendocrine cancers. *J Clin Oncol.* 2011;29: 2416–2423.
5. Krenning EP, Kwekkeboom DJ, Bakker WH, et al. Somatostatin receptor scintigraphy with [^{111}In-DTPA-D-Phe1]- and [^{123}I-Tyr3]-octreotide: the Rotterdam experience with more than 1000 patients. *Eur J Nucl Med.* 1993;20: 716–731.
6. Wild D, Schmitt JS, Ginj M, et al. DOTA-NOC, a high-affinity ligand of somatostatin receptor subtypes 2, 3 and 5 for labelling with various radiometals. *Eur J Nucl Med Mol Imaging.* 2003;30:1338–1347.
7. Wild D, Macke HR, Waser B, et al. ^{68}Ga-DOTANOC: a first compound for PET imaging with high affinity for somatostatin receptor subtypes 2 and 5. *Eur J Nucl Med Mol Imaging.* 2005;32:724.
8. Antunes P, Ginj M, Zhang H, et al. Are radiogallium-labelled DOTA-conjugated somatostatin analogues superior to those labelled with other radiometals? *Eur J Nucl Med Mol Imaging.* 2007;34:982–993.
9. Asnacios A, Courbon F, Rochaix P, et al. Indium-111-pentetreotide scintigraphy and somatostatin receptor subtype 2 expression: new prognostic factors for malignant well-differentiated endocrine tumors. *J Clin Oncol.* 2008;26:963–970.
10. Gabriel M, Decristoforo C, Kendler D, et al. ^{68}Ga-DOTA-Tyr3-octreotide PET in neuroendocrine tumors: comparison with somatostatin receptor scintigraphy and CT. *J Nucl Med.* 2007;48:508–518.
11. Buchmann I, Henze M, Engelbrecht S, et al. Comparison of ^{68}Ga-DOTATOC PET and ^{111}In-DTPAOC (Octreoscan) SPECT in patients with neuroendocrine tumours. *Eur J Nucl Med Mol Imaging.* 2007;34:1617–1626.
12. Srirajaskanthan R, Kayani I, Quigley AM, Soh J, Caplin ME, Bomanji J. The role of ^{68}Ga-DOTATATE PET in patients with neuroendocrine tumors and negative or equivocal findings on ^{111}In-DTPA-octreotide scintigraphy. *J Nucl Med.* 2010;51:875–882.
13. Ambrosini V, Tomassetti P, Franchi R, Fanti S. Imaging of NETs with PET radiopharmaceuticals. *Q J Nucl Med Mol Imaging.* 2010;54:16–23.
14. Poeppel TD, Binse I, Petersenn S, et al. ^{68}Ga-DOTATOC versus ^{68}Ga-DOTATATE PET/CT in functional imaging of neuroendocrine tumors. *J Nucl Med.* 2011;52:1864–1870.
15. Kabasakal L, Demirci E, Ocak M, et al. Comparison of ^{68}Ga-DOTATATE and ^{68}Ga-DOTANOC PET/CT imaging in the same patient group with neuroendocrine tumours. *Eur J Nucl Med Mol Imaging.* 2012;39:1271–1277.
16. Zhernosekov KP, Filosofov DV, Baum RP, et al. Processing of generator-produced ^{68}Ga for medical application. *J Nucl Med.* 2007;48:1741–1748.
17. Shastry M, Kayani I, Wild D, et al. Distribution pattern of ^{68}Ga-DOTATATE in disease-free patients. *Nucl Med Commun.* 2010;31:1025–1032.
18. Kayani I, Bomanji JB, Groves A, et al. Functional imaging of neuroendocrine tumors with combined PET/CT using ^{68}Ga-DOTATATE (DOTA-DPhe1,Tyr3-octreotate) and ^{18}F-FDG. *Cancer.* 2008;112:2447–2455.
19. Blaker H. Confidence curves and improved exact confidence intervals for discrete distributions. *Can J Stat.* 2000;28:783–798.
20. Newcombe RG. Interval estimation for the difference between independent proportions: comparison of eleven methods. *Stat Med.* 1998;17:873–890.
21. Klimstra DS, Modlin IR, Coppola D, Lloyd RV, Suster S. The pathologic classification of neuroendocrine tumors: a review of nomenclature, grading, and staging systems. *Pancreas.* 2010;39:707–712.
22. Pfannenberg C, Schraml C, Schwenzer N, et al. Comparison of [^{68}Ga] DOTATOC-PET/CT and whole-body MRI in staging of neuroendocrine tumors [abstract]. *Cancer Imaging.* 2011;11(spec no. A):S38–S39.
23. Haug A, Auernhammer CJ, Wangler B, et al. Intraindividual comparison of ^{68}Ga-DOTA-TATE and ^{18}F-DOPA PET in patients with well-differentiated metastatic neuroendocrine tumours. *Eur J Nucl Med Mol Imaging.* 2009;36: 765–770.

24. Mikkaichi T, Suzuki T, Tanemoto M, Ito S, Abe T. The organic anion transporter (OATP) family. *Drug Metab Pharmacokinet.* 2004;19:171–179.
25. Boy C, Heusner TA, Poeppel TD, et al. ^{68}Ga-DOTATOC PET/CT and somatostatin receptor (sst1-sst5) expression in normal human tissue: correlation of sst2 mRNA and SUVmax. *Eur J Nucl Med Mol Imaging.* 2011;38:1224–1236.
26. Epelbaum J, Bertherat J, Prevost G, et al. Molecular and pharmacological characterization of somatostatin receptor subtypes in adrenal, extraadrenal, and malignant pheochromocytomas. *J Clin Endocrinol Metab.* 1995;80: 1837–1844.
27. Kubota A, Yamada Y, Kagimoto S, et al. Identification of somatostatin receptor subtypes and an implication for the efficacy of somatostatin analogue SMS 201-995 in treatment of human endocrine tumors. *J Clin Invest.* 1994;93: 1321–1325.
28. Unger N, Serdiuk I, Sheu SY, et al. Immunohistochemical localization of somatostatin receptor subtypes in benign and malignant adrenal tumours. *Clin Endocrinol (Oxf).* 2008;68:850–857.
29. Lupp A, Nagel F, Doll C, et al. Reassessment of sst(3) somatostatin receptor expression in human normal and neoplastic tissues using the novel rabbit monoclonal antibody UMB-5. *Neuroendocrinology.* March 13, 2012 [Epub ahead of print].
30. Reubi JC, Kappeler A, Waser B, Schonbrunn A, Laissue J. Immunohistochemical localization of somatostatin receptor sst2A in human pancreatic islets. *J Clin Endocrinol Metab.* 1998;83:3746–3749.
31. Gugger M, Waser B, Kappeler A, Schonbrunn A, Reubi JC. Cellular detection of sst2A receptors in human gastrointestinal tissue. *Gut.* 2004;53: 1431–1436.
32. Reubi JC, Waser B, Horisberger U, et al. In vitro autoradiographic and in vivo scintigraphic localization of somatostatin receptors in human lymphatic tissue. *Blood.* 1993;82:2143–2151.
33. Ben-Shlomo A, Melmed S. Pituitary somatostatin receptor signaling. *Trends Endocrinol Metab.* 2010;21:123–133.
34. Miller GM, Alexander JM, Bikkal HA, Katznelson L, Zervas NT, Klibanski A. Somatostatin receptor subtype gene expression in pituitary adenomas. *J Clin Endocrinol Metab.* 1995;80:1386–1392.
35. Castellucci P, Pou Ucha J, Fuccio C, et al. Incidence of increased ^{68}Ga-DOTANOC uptake in the pancreatic head in a large series of extrapancreatic NET patients studied with sequential PET/CT. *J Nucl Med.* 2011;52:886–890.
36. Sasson R, Vaknin D, Bross A, Lavie E. Determination of HEPES in ^{68}Ga-labeled peptide solutions. *J Radioanal Nucl Chem.* 2010;283:753–756.